ICES Journal of Marine Science, 54: 283–299. 1997

The Arctic Ocean–Nordic Seas thermohaline system

J. Meincke, B. Rudels, and H. J. Friedrich

Meincke, J., Rudels, B., and Friedrich, H. J. 1997. The Arctic Ocean–Nordic Seas thermohaline system – ICES Journal of Marine Science, 54: 283–299.

The Arctic Mediterranean Sea is located north of the Greenland–Scotland Ridge and allows warm water from lower latitudes to penetrate beyond the Polar Circle. The northward flowing water is cooled in the Norwegian Sea and its density increases. In the Arctic Ocean the high river runoff and the net precipitation lead to a density decrease in the surface layers and heat loss at the sea surface results in the formation and maintenance of a permanent sea-ice cover. Brine ejected by freezing creates dense waters on the Arctic Ocean shelves, which sink as convecting boundary plumes into the deeper layers. In the Eurasian Basin the water column primarily reflects the interaction between the two inflows from the Norwegian Sea: through Fram Strait and over the Barents and Kara Sea and their different transformation histories. In the Canadian Basin the water transformations are dominated by the boundary convection, which makes the Canadian Basin water column different from that of the Eurasian Basin already at levels shallower than the now known sill depth of the Lomonosov Ridge. In the Greenland Sea deep-reaching, open-ocean convection occurs, partly rehomogenising the water column. The waters entering the Arctic Mediterranean are thus transformed partly into a low salinity, cold upper layer, partly into cold, dense deep waters which all re-cross the Greenland–Scotland Ridge. The dense waters sink into the deep North Atlantic to supply the North Atlantic Deep Water. A reduction of the deep convection in the Greenland Sea has recently been inferred and the Greenland Sea deep water renewal presently occurs by advection of deep waters from the Arctic Ocean. Observed changes in the temperature and salinity of the Greenland Sea Deep Water are used to estimate the vertical diffusion coefficient in the deep layers and the renewal time of the deep salinity maximum layer, which originates from deep water outflow from the Eurasian Basin through Fram Strait. A weaker convection in the Greenland Sea is found to influence primarily the deep water circulation internal to the Arctic Mediterranean. The supply of dense overflow water from the upper layers in the Greenland Sea and from the other sources is not expected to be reduced.

Key words: Arctic Mediterranean Seas, convection, thermo-haline circulation.

Received 23 February 1996; accepted 13 February 1997.

J. Meincke, B. Rudels, and H. J. Friedrich: Institut für Meereskunde der Universität Hamburg, Troplowitzstrasse 7, D-22529 Hamburg, Germany.

Introduction

The part of the Atlantic north of the Greenland–Scotland Ridge forms the Arctic Mediterranean Sea (Fig. 1). It comprises the Nordic Seas; the Greenland Sea, the Iceland Sea and the Norwegian Sea, and the Arctic Ocean. The Arctic Ocean is by far the largest component, consisting of two major basins, the Eurasian and the Canadian Basin, separated by the Lomonosov Ridge, and of shallow shelf seas: the Barents, Kara, Laptev, East Siberian, and Chukchi Sea, making up one third of its area. The Arctic Mediterranean communicates primarily with the North Atlantic over the Greenland–Scotland Ridge. A second outflow to the North Atlantic occurs through the Canadian Arctic Archipelago into Baffin Bay. An inflow takes place through the Bering Strait, directly connecting the Pacific to the North Atlantic.

The Arctic Mediterranean, like the Mediterranean, transforms and exports Atlantic Water of lower density entering from the adjacent ocean into high density intermediate and deep waters. However, because of the high precipitation it also, like enclosed seas such as the Baltic and the Black Sea, forms and exports surface water of lower salinity and density.

We shall examine the deep and bottom water renewal of the Greenland Sea and put it into the context of the Arctic Ocean–Nordic Seas thermohaline system and also

1054–3139/97/040283+17 $25.00/0/jm970229

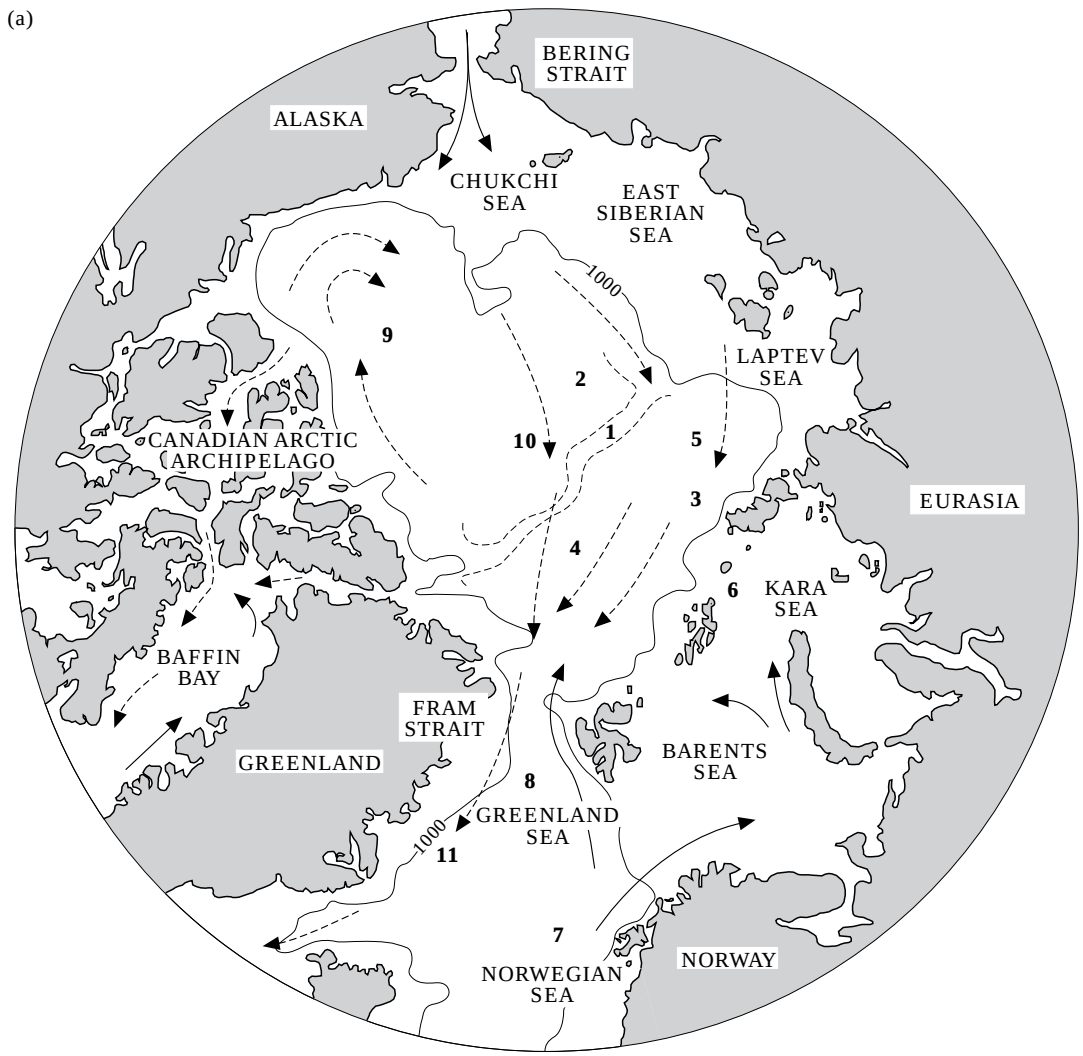

Figure 1. Map of the Arctic Mediterranean: (a) numbers indicate the most prominent features of the bathymetry and the circulation. (1) Lomonosov Ridge, (2) Canadian Basin, (3) Eurasian Basin, (4) Amundsen Basin, (5) Gakkel Ridge, (6) St Anna Trough, (7) Norwegian Atlantic Current, (8) West Spitsbergen Current, (9) Beaufort Gyre, (10) Transpolar Drift, (11) East Greenland Current – the known surface circulation is also depicted. Full arrows: waters of Atlantic/Pacific origin. Broken arrows: waters of Arctic origin. Continued on following page.

try to evaluate the importance of the Greenland Sea deep convection for the formation of North Atlantic Deep Water. In this section we summarise the main features of the Arctic Mediterranean using freely the information and insights available in recent reviews (Coachman and Aagaard, 1974; Aagaard *et al.*, 1985; Aagaard and Carmack, 1989; Carmack, 1990; Aagaard and Carmack, 1994; Rudels, 1995).

The poleward extension of the North Atlantic allows warm and saline Atlantic water to flow northward along the Norwegian slope and eventually enter the Arctic Ocean. These warm waters transfer their heat to the atmosphere resulting in a warmer climate in north-western Europe than at corresponding latitudes elsewhere. As the water column cools the upper mixed layer becomes deeper and denser.

The atmospheric circulation delivers a considerable excess of fresh water to this region through direct net precipitation and through a large river runoff. This input of fresh water counteracts the effects of cooling and the poleward density increase of the surface water is retarded and finally changes into a density decrease. A shallow, low density surface layer is formed. The presence of this layer inhibits the upward transfer of heat from the deep ocean to the atmosphere. The limited amount of sensible heat stored in the surface layer is lost by cooling and its temperature falls to freezing. Fresh water is then removed from the mixed layer as ice forms

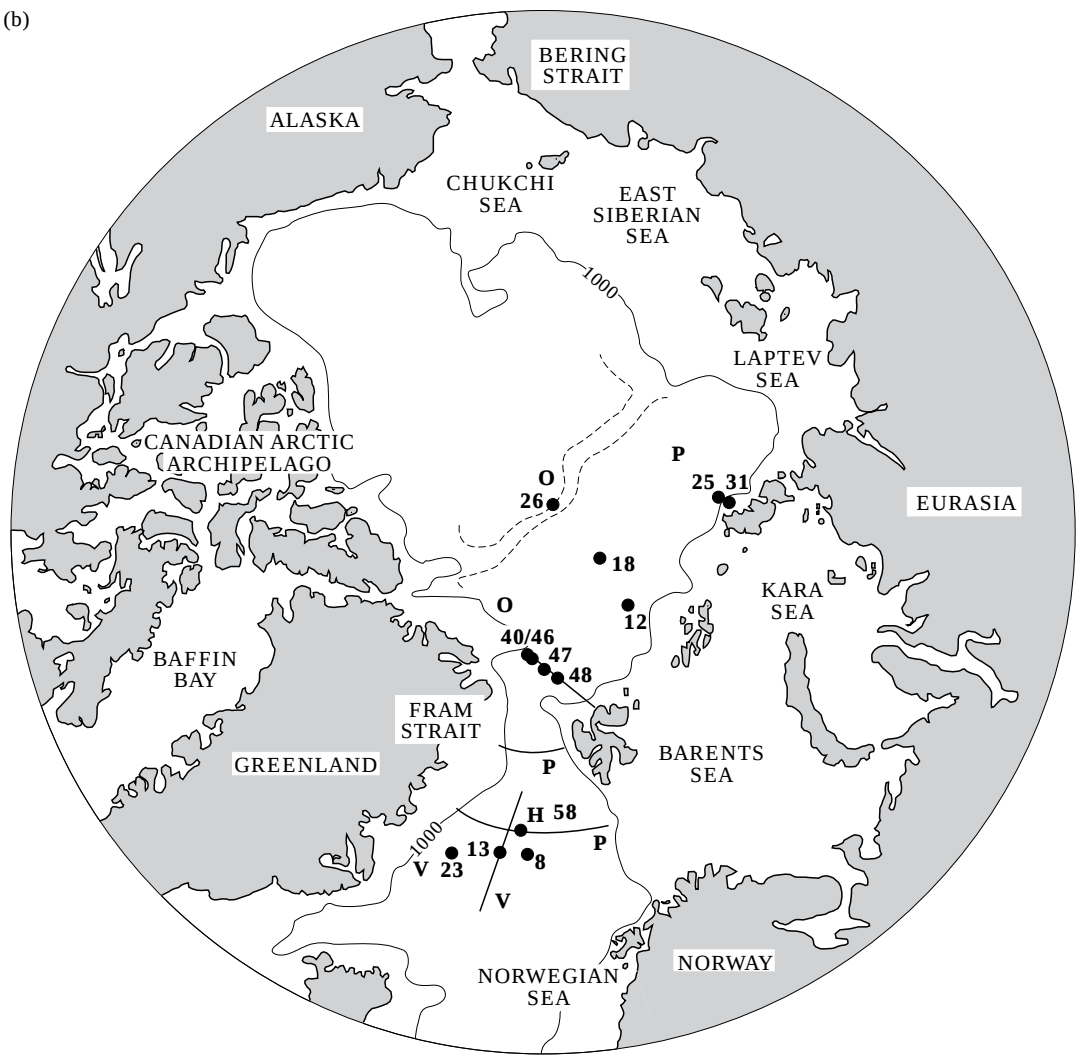

Figure 1. (b) Indicates the positions of the discussed stations and sections.

and its salinity (and density) now increases rapidly. The ice cover, however, insulates the ocean and reduces the heat loss and thereby lowers the ice formation rate. The density increase of the mixed layer slows down.

When the fresh water fraction in the surface layer is large, as is the case in the Arctic Ocean, the oceanic heat flux is greatly suppressed and a permanent ice cover is maintained. The fresh water fraction in the Greenland Sea surface layer is much smaller, and the stability at its base is small because of brine ejection in winter and thus entrainment and heat flux from the layers below become important. The density of the mixed layer then increases not only by brine ejection but also by the incorporation of denser water from below, while the entrained heat limits the growth of the ice cover. The heat loss to the atmosphere remains large. Deep convection and the formation of dense water masses may then result.

The broad, shallow shelves of the Arctic Ocean are also potential sources for dense water. The shelves are ice free in summer and the thinner ice cover in winter enhances ice production and brine ejection. The saline water accumulates at the bottom, increasing the density of the shelf bottom water. In areas where the ice is persistently removed, e.g. in polynyas in the lee of islands, the ice production remains large and the bottom waters attain high densities. When the shelf bottom water reaches the shelf break, it sinks down the continental slope to renew the deeper layers (Nansen, 1906).

The waters of the Arctic Mediterranean are considered to be ultimately derived from two sources, Atlantic Water crossing the Greenland–Scotland Ridge and fresh water added through net precipitation and river runoff.

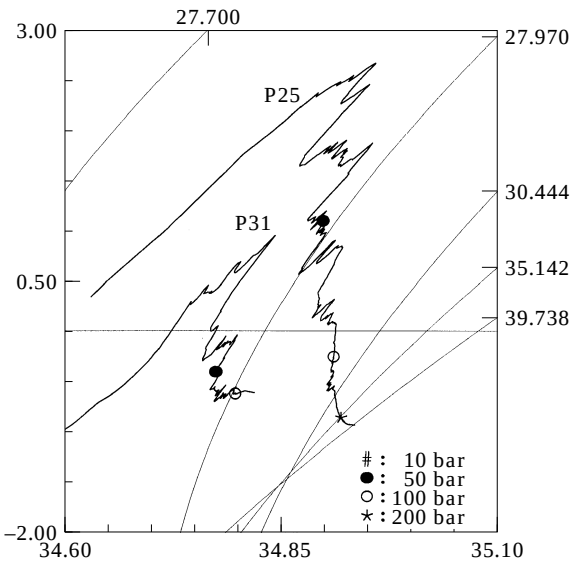

Figure 2. Θ–S curves for two stations: P25 81°08′N 105°31′E, P31: 80°47′N 103°26′E. Taken by FS Polarstern in 1995 north of the Laptev Sea (ARKXI/1), showing the two inflow branches. The isopycnals shown in the diagram are σ_0=27.7, σ_0=27.97, $\sigma_{0.5}$=30.444, σ_2=35.142, σ_3=39.738.

The inflow through the Bering Strait and the outflow through the Canadian Arctic archipelago are of similar magnitude and are assumed to compensate each other. They are therefore neglected in this description. In the following section the Atlantic Water is followed from its northward crossing of the Greenland–Scotland Ridge along its route around the Nordic Seas and the Arctic Ocean and its splittings, mergings and transformations are discussed. In the Arctic Ocean the causes of the different water mass characteristics in the Eurasian and the Canadian basins are examined. In the Greenland Sea the influences of a low salinity surface layer and sea-ice on deep convection are considered. The strength of turbulent mechanical mixing in the deep interior and the rate of the advective replacement of the deeper layers in the absence of deep convection are assessed. In the final section recently observed changes in the Arctic Mediterranean are discussed and their possible implications for the climate and the global thermohaline circulation are considered.

The data used are, except those from one station of the Hudson 1982 expedition, obtained from cruises where at least one of us has participated actively. Most of the observations have been published and discussed earlier. One notable exception is the Polarstern ARKXI/1 cruise in 1995 to the Laptev Sea (Fig. 2).

The Atlantic inflow

Atlantic Water crosses the Greenland–Scotland Ridge and flows northward along Norway as the Norwegian Atlantic Current. The inflow is estimated to 5–8 Sv (Worthington, 1970; McCartney and Talley, 1984), and the strong heat loss in the Norwegian Sea leads to winter convection down to 600–800 m. When the current reaches the latitude of the Bear Island Channel it splits. One part enters, together with the Norwegian Coastal Current, the Barents Sea while the rest continues as the West Spitsbergen Current toward Fram Strait. Here the current again splits. The smaller part, about 1 Sv (1×10^6 m^3 s^{-1}) (Rudels, 1987; Bourke *et al.*, 1988) enters the Arctic Ocean while the rest recirculates in several branches toward the west (Quadfasel and Meincke, 1987; Quadfasel *et al.*, 1987; Rudels, 1987).

North of Svalbard the Atlantic Water encounters and melts sea-ice and a low salinity surface layer is formed (Untersteiner, 1988; Steele *et al.*, 1995). In winter, freezing and haline convection transform this surface water into a more than 100 m deep mixed layer (Rudels *et al.*, 1996). The lower part of the mixed layer appears to follow the Atlantic Water as it flows as a boundary current eastward along the continental slope. Heat is transferred upward into the lower part of the surface layer by turbulent mixing and by double-diffusive convection. This heat is lost to the atmosphere in winter as the summer ice melt is replaced by freezing and the mixed layer is again homogenised down to the Atlantic Layer. The Atlantic Layer itself is largely decoupled from the atmosphere and its main transformations occur through interactions with plumes of dense water originating from the Barents Sea shelf, which sink into and cool the Atlantic Layer (Rudels, 1986; Schauer *et al.*, 1997).

The inflow to the Barents Sea is estimated to 2–3 Sv (Rudels, 1987; Blindheim, 1989). It is subject to stronger interactions with the atmosphere and its density range increases. The entire water column is cooled but the upper part becomes less saline and less dense due to mixing with water from the Norwegian Coastal Current, by net precipitation and by ice melt. The lower part becomes denser and occasionally also more saline by cooling and by the incorporation of brine-enriched water formed over shallower areas of the Barents Sea (Nansen, 1906; Midttun, 1985; Quadfasel *et al.*, 1992). The main outflow, about 2 Sv, passes between Franz Josef Land and Novaya Zemlya (Loeng *et al.*, 1993) and sinks down the St Anna Trough into the Arctic Ocean. The two inflow branches meet and partly remerge north of the Kara Sea and continue eastward (Rudels *et al.*, 1994; Schauer *et al.*, 1997).

Water transformations and circulation in the Arctic Ocean

Further to the east, beyond the Kara Sea, the large river runoff leads to an input of low salinity shelf water to the central basins above the water previously homogenised

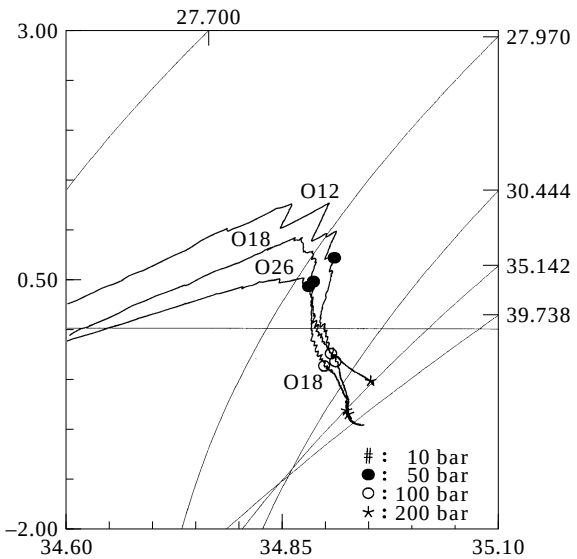

Figure 3. Θ–S curves for three stations taken by IB Oden in 1991. O12: 86°36′N 055°16′E over the Nansen–Gakkel Ridge, O18: 88°11′N 098°47′E in the Amundsen Basin and O26: 88°01′N 163°21′E in the Makarov Basin. Note the cold intermediate layer in the Amundsen Basin and the warmer, more saline deep and bottom water of the Makarov Basin. The same isopycnals are shown as in Figure 2.

by winter convection. The smaller convection depth resulting from the lower surface salinity creates a shallow Polar Mixed Layer and a halocline between the Polar Mixed Layer and the Atlantic Layer (Rudels *et al.*, 1996), which only can be replenished by injections of denser brine-enriched water from the shelves (Aagaard *et al.*, 1981).

The circulation of the Polar Mixed Layer in the Canadian Basin is anticyclonic and dominated by the wind-driven Beaufort Gyre. The Transpolar Drift moves ice and low salinity water from the gyre across the Lomonosov Ridge toward the Fram Strait. The Siberian Branch of the drift flows north from the Laptev Sea but then veers toward Fram Strait.

The processes transforming the deeper layers of the Arctic Ocean can be deduced by examining profiles of potential temperature Θ and salinity S and Θ–S curves from different parts of the Arctic Ocean. They also give some hints about the circulation pattern. The two stations shown in Figure 2 were taken by FS Polarstern in 1995 north of the Laptev Sea: for station positions see Figure 1(b). The one closest to the continental slope reveals the cold, low salinity water of the Barents Sea branch, while the other station located further into the basin is dominated by the warmer, more saline Fram Strait branch.

In Figure 3 three profiles from a section occupied by IB Oden in 1991 are shown, one from the Makarov Basin, one from the Amundsen Basin and one from above the Nansen–Gakkel Ridge. The temperature maximum is lowest in the Makarov Basin and highest over the Nansen–Gakkel Ridge. All curves display inversions. The strongest are found in the Atlantic Layer but they are also seen in the intermediate layers. The inversions suggest that the Atlantic core has interacted with shelf water at the continental slope and their presence over the Nansen–Gakkel Ridge and in the Amundsen Basin is an indication that the Atlantic core here is returning toward the Fram Strait (Quadfasel *et al.*, 1993). The same conclusion was reached by Anderson *et al.* (1994) and Rudels *et al.* (1994), who also noticed that the layers below the Atlantic core were colder in the Amundsen Basin than in the Makarov Basin and over the Nansen–Gakkel Ridge. They proposed that the cooling and the inversions observed in the Eurasian Basin were due to the merging of the two Atlantic inflows, which then would mainly be recirculating in the Eurasian Basin. The Fram Strait branch would dominate over the Nansen–Gakkel Ridge and the Barents Sea branch in the Amundsen Basin. The Canadian Basin would, above 1700 m, be supplied mainly by the boundary current crossing the Lomonosov Ridge north of Siberia carrying mostly waters of the Barents Sea branch.

The fact that the Makarov Basin water column is warmer and more saline than the Eurasian Basin water column below the Atlantic Layer indicates, since no other heat source is available for the Canadian Basin, that dense waters from the shelves partly sink into and cool, partly pass through the Atlantic Layer entraining warmer Atlantic Water. When the plumes then enter the water column at their terminal density levels they have redistributed Atlantic Water downward increasing the temperature of the deeper layers. The higher salinity is caused by the higher shelf salinities required for the slope convection to reach the deepest levels (Rudels *et al.*, 1994; Jones *et al.*, 1995).

When the slope convection is below the temperature maximum it no longer cools but heats the water column. This change appears to occur at about 1300 m, as is seen if we compare the water columns from the Amundsen and Makarov Basins. This is close to the value often given for the sill depth of the Lomonosov Ridge (e.g. Carmack, 1990), which was actually deduced from the differences in temperature between the two basins (Worthington, 1953). These considerations then suggest that the layer between 1300 and 1700 m has higher temperature than the corresponding layer in the Amundsen Basin not because, as has earlier been believed, the colder Amundsen Basin water cannot cross the Lomonosov Ridge but because the water of the boundary current entering the Canadian Basin at these levels is heated by the slope convection.

The Makarov Basin water column has between 2300 and 3200 m (Fig. 3) an isohaline layer with temperature

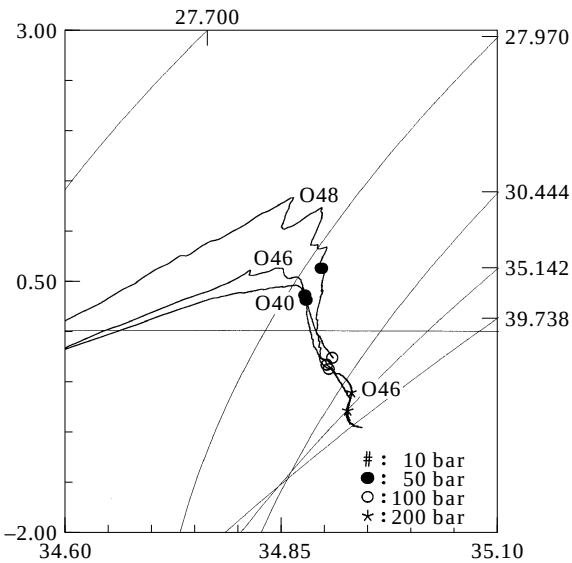

Figure 4. Θ–S curves for three stations: O40: 85°18′N 014°09′W, O46: 84°36′N 014°12′W, O48: 83°59′N 000°16′W. Taken by IB Oden in 1991 between the Morris Jesup Plateau and the Nansen–Gakkel Ridge. The differences in temperature and salinity reflect the different history of the outflowing waters. The same isopycnals are shown as in Figure 2.

slowly decreasing with depth above the 800 m deep isothermal and isohaline bottom layer. Such a temperature decrease cannot be generated by slope convection because of the entrainment of warmer intermediate water into the sinking plumes but could be caused by a spillover of colder Amundsen Basin water through deeper gaps in the central part of the Lomonosov Ridge (Jones *et al.*, 1995). By contrast the bottom water of the Eurasian Basin has almost constant temperature but the salinity increases with depth suggesting that the deepest levels here are predominantly influenced by brine-enriched water either from the shelves or from the St Anna Trough inflow.

The intermediate depth and deep waters of the Canadian Basin recross the Lomonosov Ridge mainly as a boundary current north of Greenland and they converge north of the Fram Strait with the waters returning along the Amundsen Basin and the Nansen–Gakkel Ridge. The characteristics of the Arctic Ocean water column as it is about to exit through Fram Strait are seen in Figure 4 where again the Θ–S curves from three stations taken at the Morris Jesup Plateau (O 40), in the Amundsen Basin (O 46) and over the Nansen–Gakkel Ridge (O 48) are shown. The deep water from the Canadian Basin is seen as a salinity maximum at 1800 m (O 46). This maximum is also observed further to the east in the Amundsen Basin (Fig. 3, stn. O 18). The different sources of the Atlantic, intermediate, and deep waters give large ranges of temperature and salinity, especially for the Atlantic Layer, where the temperature extends from close to 0 in the thermocline to above 1.5°C for the maximum above the Nansen–Gakkel Ridge. The salinity of the Atlantic Layer ranges from below 34.7 in the thermocline to a weak maximum of above 34.9 again found above the Nansen–Gakkel Ridge (O 48), where, in contrast to the other stations, strong interleaving can still be seen.

In the Fram Strait the Arctic Ocean outflow in the East Greenland Current encounters the recirculating waters of the West Spitsbergen Current. The temperature of the Atlantic Layer of the East Greenland Current then increases while the salinity and temperature of the layers below are reduced. These changes are clearly seen on the potential temperature and salinity sections. In Figure 5 the Oden section between the Morris Jesup Plateau and Svalbard is shown together with Polarstern sections in the Fram Strait along 79°N and across the Greenland Sea along 75°N.

Above the Greenland continental slope the temperature and salinity of the Atlantic Water increase between the northern section and the Fram Strait (Fig. 5a, b) because of the recirculating West Spitsbergen Current. At 75°N the temperature maximum at the slope is less than 1.5°C, and the high temperatures and salinites of the recirculating Atlantic Water have largely been removed, either by cooling from above or by isopycnal mixing with waters from the central Greenland Sea (Strass *et al.*, 1993). A further possibility is that a part of the Atlantic Water has been deflected by the Hovgaard Fracture Zone eastward into the Boreas Basin north of the Greenland Sea. The high salinity characteristics of the Arctic Ocean deep waters are prominent at the deeper part of the Greenland continental slope, in the Fram Strait (Fig. 5b) as well as in the Greenland Sea (Fig. 5c). This has been noticed earlier (Rudels, 1986; Aagaard *et al.*, 1991; Buch *et al.*, 1992, 1996).

Convective and advective contributions to the Greenland Sea water column

The characteristics of the Greenland Sea water column are best appreciated by comparing them with those of the Arctic Ocean. Figure 6 shows one Θ–S curve from the Arctic Ocean outflow and two Θ–S curves from the Greenland Sea, one from the Greenland slope, the other from the central gyre. The impression from the sections shown in Figure 5 are reinforced. The waters on the continental slope have distinct Arctic Ocean characteristics. The stable Θ–S slope of the upper Polar Deep Water, uPDW, (Rudels *et al.*, 1994), the intermediate salinity maximum originating from the Canadian Basin outflow, CBDW, and the deep salinity maximum deriving from the Eurasian Basin, EBDW, are identified. The upper 800–1000 m in the central part of the Greenland

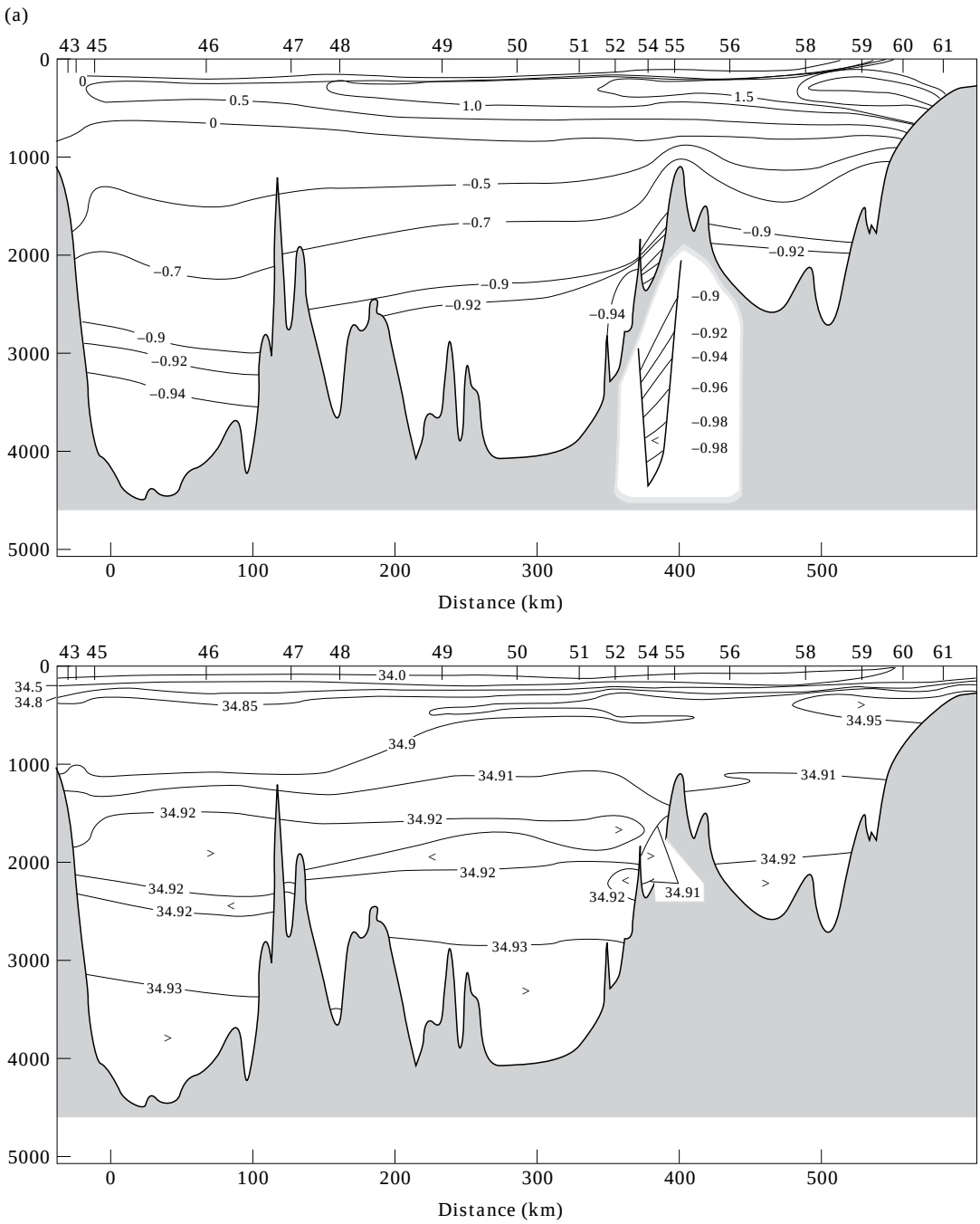

Figure 5. Three potential temperature and salinity sections across the Arctic Ocean outflow. (a) Between Morris Jesup Plateau and Svalbard occupied by IB Oden in 1991 (from Anderson *et al.*, 1994). Continued on following pages.

Sea is occupied by cold, locally formed, Arctic Intermediate Water, AIW. Below the AIW a temperature maximum and a deep salinity maximum allows us to recognise the presence of the denser Arctic Ocean deep waters (CBDW and EBDW) also in the central part of the Greenland Sea basin.

The flow of Arctic Ocean deep waters in the East Greenland Current bifurcates at the Jan Mayen Fracture Zone (Aagaard *et al.*, 1991). Part of the boundary current crosses the ridge (Buch *et al.*, 1992, 1996) while the rest turns eastward as is seen on the north–south section shown in Figure 7. The salinity maximum at

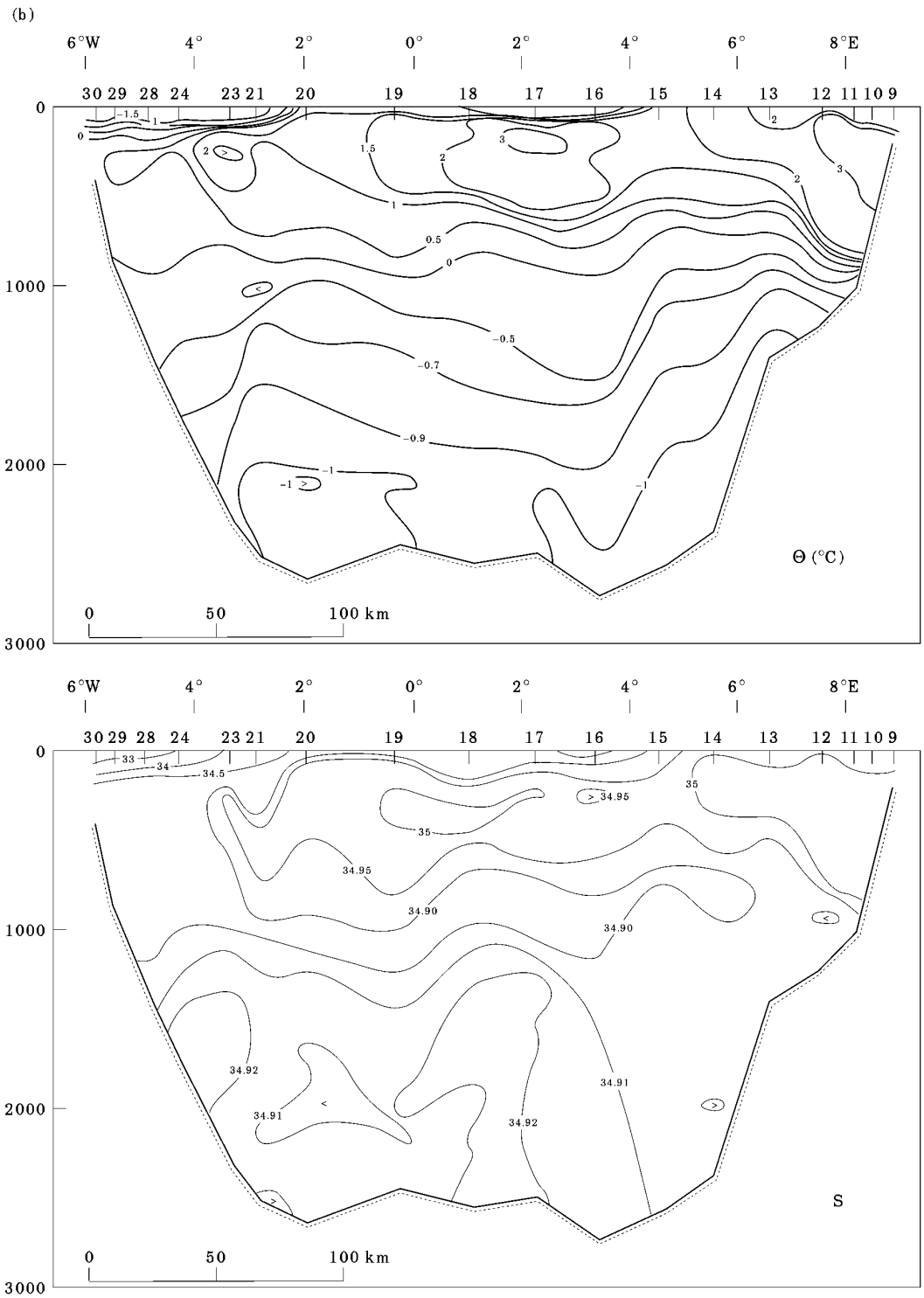

Figure 5. (b) Along 79°N in Fram Strait occupied by FS Polarstern in 1993 (ARK IX/1).

the southern rim extends from 1000 to 2000 m and indicates that both CBDW and EBDW take part in the eastward circulation along the southern rim. The upper 800 to 1000 m are in the central part of the Greenland Sea occupied by cold, locally formed AIW. Below this layer a temperature maximum and a deep

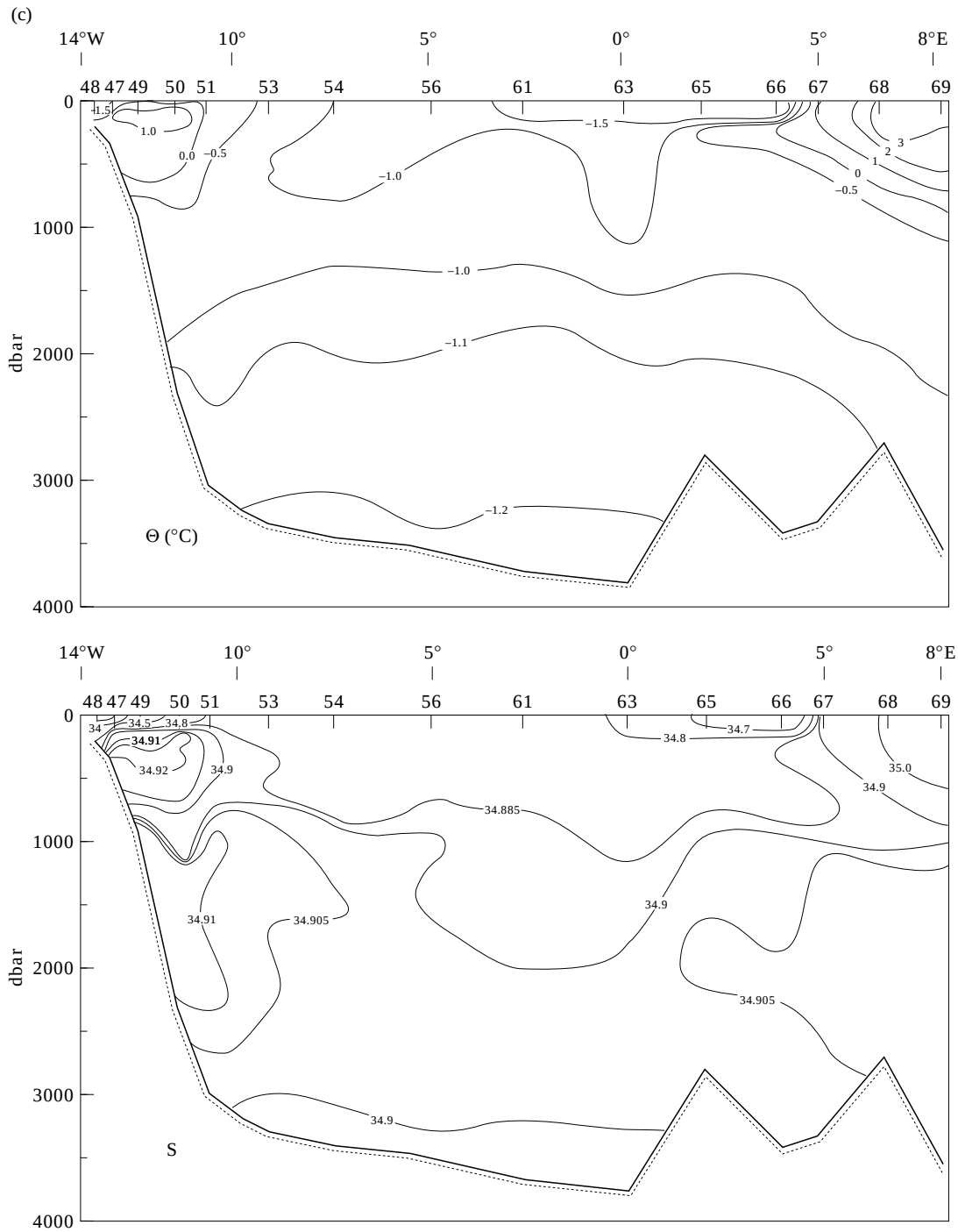

Figure 5. (c) Along 75°N across the Greenland Sea occupied by FS Polarstern in 1993 (ARK IX/1).

salinity maximum indicate the presence of the denser Arctic Ocean deep waters (CBDW and EBDW) also in the central part of the Greenland Sea basin. The Arctic Ocean deep waters thus appear to move around the Greenland Sea gyre while they gradually penetrate towards its centre (Rudels *et al.*, 1993; Meincke and Rudels, 1996).

A decrease in the deep convection activity in the Greenland Sea has recently been observed (GSP-Group, 1990; Rhein, 1991; Schlosser *et al.*, 1991). Convection

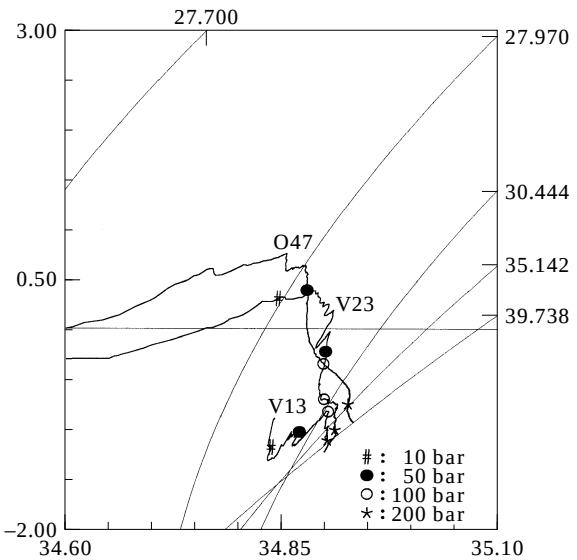

Figure 6. Θ–S curves for three stations: O47: 84°13′N 002°30′W, taken in the outflow area north of Fram Strait by IB Oden in 1991. V23: 73°00′N 011°42′W on the Greenland Slope and V13: 74°00′N 006°30′W in the central Greenland Sea gyre. Taken by FS Valdivia in 1993. Note the similar density of the deep salinity maximum in the Greenland Sea and the Eurasian Basin Deep Water and the similar density of the upper salinity maximum of the Canadian Basin Deep Water and the temperature maximum in the central Greenland Sea. The same isopycnals are shown as in Figure 2.

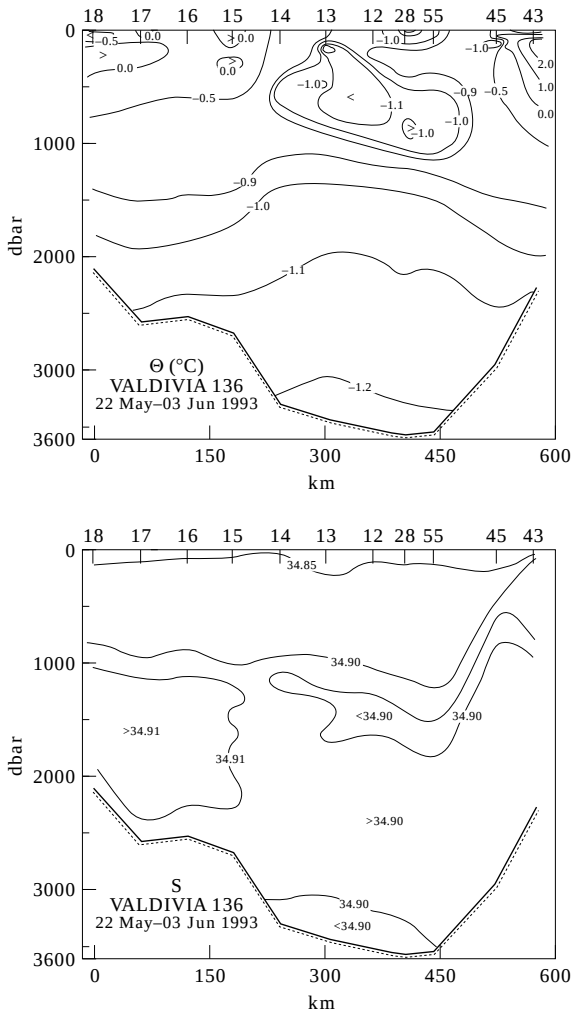

Figure 7. North–south potential temperature and salinity sections across the central Greenland Sea from stations occupied by FS Valdivia in 1993 (Valdivia cruise 136) showing the presence of Arctic Ocean waters on the southern rim of the Greenland Sea.

has been limited to about 1000 m and AIW has been formed but the Greenland Sea Deep Water, GSDW, has not been ventilated by local convection. This change can be seen in Figure 8 which shows the Θ–S curves from the central Greenland Sea from 1982 and 1993. In 1982 the temperature maximum was much colder, indicating that the upper salinity maximum of the CBDW, if it penetrated into the central gyre at all, was transformed into GSDW. In more recent winters the convection has been shallower and the presence of the CBDW has become more prominent.

By GSDW we understand here the water mass found below the inflexion point (in a Θ–S diagram) in the thermocline between the temperature minimum of the AIW and the temperature maximum of the CBDW. It comprises three different water masses: the CBDW, the EBDW and the input from local convection. Its Θ–S characteristics are not constant but vary depending upon which source is the most prominent one.

By GSBW we shall understand the part of GSDW which cannot be renewed by advection from the Arctic Ocean but only by local convection. In the absence of convection it will be diluted and slowly removed by turbulent mixing. In essence the GSBW is the part of the water column below the deep salinity maximum related to the EBDW. If the deep maximum reaches the bottom we consider the GSDW to be absent.

The invasion of Arctic Ocean deep waters into the Greenland Sea is likely to be related to the present day weak convection (Meincke *et al.*, 1992). A higher convection activity would increase the density of the central gyre and obstruct the penetration of the Arctic Ocean deep waters towards the centre. When they do reach the central parts it will be at shallower levels as is seen from the location of the deep salinity maximum in 1982 and 1993 (Fig. 10b).

What are the reasons for this weaker convective activity and are there optimal conditions for deep convection and deep water renewal in the Greenland Sea? One obvious cause would be that a temperature increase

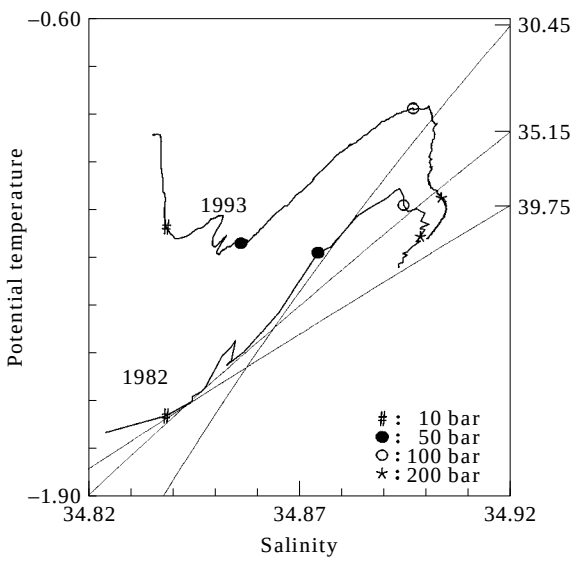

Figure 8. Θ–S curves for stations from the central Greenland Sea gyre. H58: 75°02′N 005°11′W taken by RV Hudson in 1982 (Clarke *et al.*, 1984) and V8: 74°00′N 004°20′W, taken by FS Valdivia in 1993 (Cruise 136) showing the increase in salinity and temperature of the Greenland Sea Deep Water. The isopycnals $\sigma_{0.5}=30.45$, $\sigma_2=35.15$, $\sigma_3=39.75$ are shown.

has occurred, either locally over the Greenland Sea or regionally in the Arctic, leading to smaller ice formation and more fresh water in the surface layer, or in the North Atlantic bringing warmer Atlantic Water into the Arctic Mediterranean.

Our concern here is not the history of the local and regional climate but rather which Θ–S characteristics of the Greenland Sea water column are most favourable for deep convection and dense water formation. Essentially two possibilities exist (Aagaard and Carmack, 1989). One requires that the upper waters are dominated by saline Atlantic Water and that the freshwater content in the mixed layer is small. This leads to a short period of ice formation and a thermal convection regime is quickly established, bringing already saline water into the deep. The second view suggests that ice formation leads to a more rapid increase in density in the upper layer and provided that the created ice does not become too thick a high heat loss will persist and large densities are reached in the surface mixed layer by brine ejection, permitting it to sink into the deep by haline convection. For reviews of ocean deep convection we refer to Carmack (1986), Killworth (1983), and Rudels (1993).

Convection occurs on small scales and its detailed description involves non-linear dynamics and the effects arising from the non-linear equation of state for sea water (Jones and Marshall, 1993; Garwood *et al.*, 1994; Backhaus, 1995). Moreover, the presence of sea-ice greatly complicates the behaviour of even the simplest energy balance mixed layer model and much depends upon how the interactions between heat loss to the atmosphere and entrained heat from below and between freezing and ice melt are prescribed (Lemke, 1987; Houssais, 1988; Houssais and Hibler, 1993; Walin, 1993; Visbeck *et al.*, 1995).

Lemke (1987) and Houssais and Hibler (1993) assume that all heat entrained from below first goes to ice melt. After this the surface heat balance with the atmosphere is closed by renewed ice formation. In a two-layer one-dimensional energy balance model (Niiler and Kraus, 1977) this, as well as any assumption that decouples the ice melt from the freshwater content in the mixed layer, would lead to the removal of the density step below the mixed layer while sea-ice is still present, and to the convection of the mixed layer into the deep.

Walin (1993) and Visbeck *et al.* (1995) consider the net ice melt (or freezing) resulting from a balance between entrained heat and heat loss to the atmosphere. This relates the buoyancy flux caused by the ice melt directly to the freshwater content in the mixed layer. The stability at the base of the mixed layer will then not go to zero before all the ice has melted. When the ice is gone a deep thermal convection is established.

If convection out of the mixed layer occurs when ice is still present we would expect the reformation of a low salinity mixed layer after the convection event as the warmer deep waters are brought close to the sea surface and the ice. This appears to have taken place in the winter 1987–1988. One station in the central Greenland Sea showed an almost homogenous cold and low salinity 1250 m deep water column capped by a low salinity colder surface layer (Rudels *et al.*, 1989 and Fig. 9a). By contrast the three successive temperature and salinity profiles obtained from the same position in the winter 1988–1989 and shown in Figure 9(b) (GSP-Group, 1990) do not have such a low salinity surface layer and they suggest deep, homogenising thermal convection.

Roach *et al.* (1993) and Visbeck *et al.* (1995) describe the evolution of the mixed layer and the ice cover in the period before these stations were taken. From their observations it appears that some ice was left when the convection started and that the ice melted when warmer water was brought to the surface from below. Two events with colder water passing downwards were recorded before a gradual deepening and cooling of the mixed layer was established. This would support a picture where first an event of haline convection occurs emptying the mixed layer and bringing the underlying water to the surface. The subsequent ice melt creates a low salinity surface layer with temperature above freezing and a weak stability at its base. Entrainment will cause the ice to melt before the freezing point is reached again and with further cooling the mixed layer becomes unstable and a second, cold thermal convection event occurs before the gradually deepening thick mixed layer seen in Figure 9(b) is established. However, the evidence

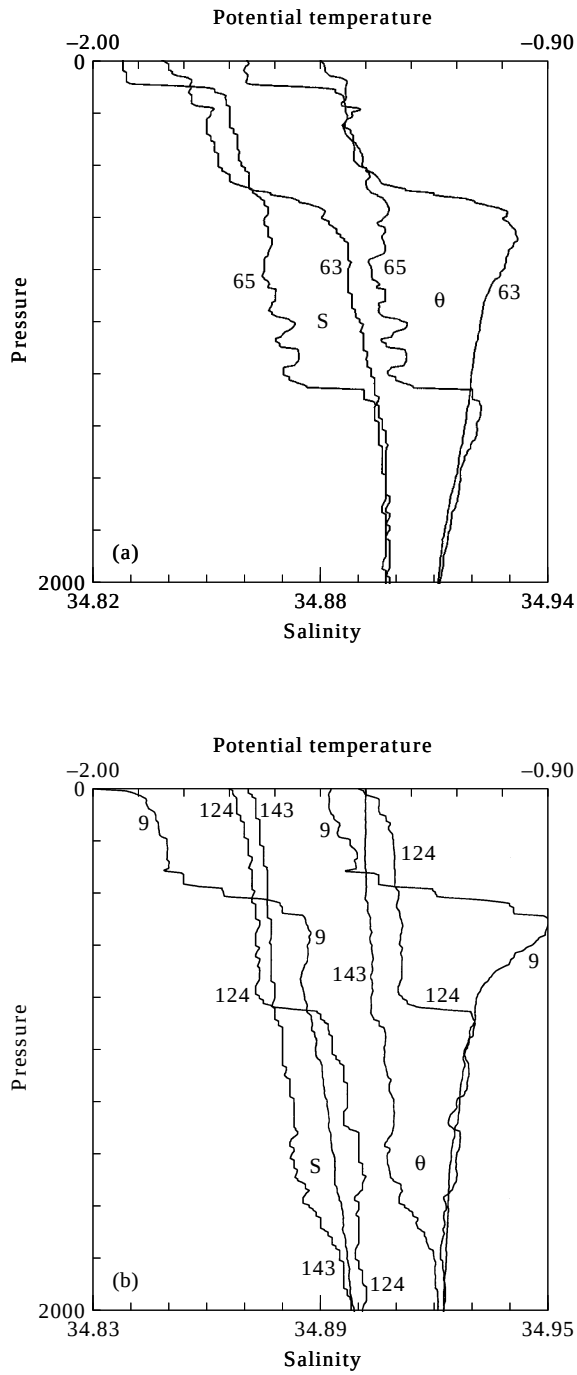

Figure 9. Temperature and salinity profiles from the central Greenland Sea. (a) Two neighbouring stations from February 1988 taken on the RV Valdivia cruise 67. On the colder, less saline station the low salinity surface mixed layer suggest a previous haline convection down to 1200 m (also shown by Rudels *et al.*, 1989). (b) Three successive stations taken in winter 1989 on the Valdivia cruise 78. No low salinity surface layer is observed and the deepening is primarily due to thermal convection down to 2000 m (also shown by the GSP-Group, 1990).

for such a scenario is not conclusive. Roach *et al.* (1993) favour an initial convection out of the mixed layer and a subsequent ice melt while the mixed layer model applied by Visbeck *et al.* (1995) gives, with a prescribed ice export, the removal of the ice before the deep convection begins.

The latest observed and reported deep convection events have been limited to 2000 m and have then, if not earlier, entered the thermal convection stage (GSP-Group, 1990). In the winter of 1994 no ice was formed in the central Greenland Sea and the pure thermal convection only reached 600 m (D. Quadfasel, pers. comm.). Thermal convection might then not be capable, in spite of the high heat loss taking place through the open ocean surface, to create densities high enough to renew the bottom water. If, by contrast, the convection remains longer in its haline phase, several cold, haline convection events could occur. Higher densities could then be reached and injections of cold water into the underlying water column would take place. Such a situation is favoured if the intermediate waters are cold and only a small amount of warm Atlantic Water is present in the central gyre, and the freshwater content in the mixed layer is high enough to maintain the ice cover over a longer period. The support for such a mechanism is, however, at best a combination of negations – no deep, haline convection has been observed and no renewal of the bottom water has occurred.

When really deep convection is active the water mass below the deep salinity maximum is renewed and the salinity maximum is observed high in the water column. As the convection becomes weaker the salinity maximum is displaced downward (Fig. 10b). This could partly be due to an outflow of the deeper layers but it also implies that the doming of the isopycnals in the central Greenland Sea gyre weakens when the deep convection ceases. The doming of the density surfaces of the Greenland Sea would then not only be a wind-driven phenomena (Helland-Hansen and Nansen, 1909) but also influenced by the convection. During deep convection periods some of the denser GSDW was found to exit through the rift north of Jan Mayen (Sælen, 1986). In recent years the outflow through this gap has been replaced by a weak inflow from the Norwegian Sea (S. Østerhus, pers. comm.).

Estimates of vertical diffusion and deep water renewal

The absence of deep convection in the Greenland Sea has led to a decrease in density but an increase in salinity of the bottom water, while the density of the salinity maximum has remained the same in spite of an increase in salinity. This implies that the salinity maximum is advectively renewed by the Arctic Ocean deep outflow while the layer below is tranformed only by turbulent

vertical diffusion. This should make it possible to estimate a turbulent vertical diffusion coefficient for the deepest layer. The estimates below are, as should be obvious from the crude assumptions made, very approximate and are to be considered as exploratory.

The salinity of the salinity maximum has increased from 34.896 to 34.905 and it has been displaced downward from 1600 to 2400 m between 1982 and 1993. During the same period the salinity of the GSBW, the layer with constant salinity below the salinity gradient, has risen from 34.892 to 34.900 and its height decreased from 1000 to 400 m. The thickness of the salinity gradient layer below the salinity maximum has changed from 1000 to 800 m (Fig. 10b). The mean vertical salinity gradient between the bottom water and the salinity maximum is then estimated to $\partial S/\partial z = 4.4 \cdot 10^{-6}\ m^{-1}$. Taking the mean thickness H of the GSBW to be 700 m between 1982 and 1993 the flux of salt into the bottom layer in those years can be found from:

$$\frac{\Delta S_B H}{t} = \kappa_v \frac{\partial S}{\partial z} \tag{1}$$

where $\Delta S_B = 0.007$ is the change in salinity in the bottom layer and t is 11 years. This leads to

$$\kappa_v \approx 3.7 \cdot 10^{-3}\ m^2\ s^{-1} \tag{2}$$

This value is very high compared to the $10^{-4}\ m^2\ s^{-1}$ obtained by Munk (1966) and is especially high in comparison with $\kappa_v = 10^{-5}\ m^2\ s^{-1}$ found by Ledwell *et al.* (1993) in the thermocline of the subtropical Atlantic. However, the Greenland Sea is weakly stratified, quite small and is subject to a large energy input at the surface from wind and convection, which might radiate into the deep and enhance the mixing. Moreover, the currents may interact with the bathymetry, dissipate and generate boundary mixing.

As a control we also derive, in a similar manner, the turbulent diffusion coefficient for heat which should be the same. The temperature difference between the salinity maximum layer and the Greenland Sea Bottom Water was 0.12°C in 1982 and 0.08°C in 1993 giving an average of 0.10°C. Using the same thickness for the gradient and bottom layers as above and the observed increase of $\Delta T_B = 0.103$°C in the bottom water we get $\kappa_v = 2.1 \cdot 10^{-3}\ m^2\ s^{-1}$, a little more than half but reasonably close to the value obtained for the salt diffusion.

A further possibility to increase the mixing would be by double-diffusive convection. Carmack and Aagaard (1973) and McDougall (1983) have invoked the double-diffusive transfer across diffusive interfaces as a mechanism for the formation of GSDW. The cooling of the surface layer in winter keeps the stability ratio small and a constant ratio of the upward heat and salt fluxes can be assumed. The density increase associated with the heat loss is larger than the density decrease due to the corresponding salt flux. Atlantic Water, which penetrates toward the centre of the gyre, then becomes denser. It was supposed to have attained the density of the GSDW when it reaches the centre and would then convect into the deep.

Here we are concerned with processes occurring below the salinity maximum and the only possible double-diffusive transfer would be saltfinger transports from the salinity maximum to the bottom layer. However this cannot be the dominating mechanism since double-diffusive convection transports density downward. The density of the bottom layer should then increase, not decrease, as is observed. Saltfinger fluxes could, however, add to the turbulent fluxes of salt and heat in such a manner that the estimate of the turbulent diffusivity coefficient for salt becomes larger than that for heat. Such a difference was found in the estimate above but we believe that this difference is rather due to the sparse data and to the crude model than an effect of saltfinger fluxes.

For the 1982 Hudson data we have used the CTD values given in the Data Report (Clarke *et al.*, 1984). These values were later subject to a revision upwards (Aagaard *et al.*, 1991). However, the Meteor observations from the same year indicate that the GSBW is less saline than 34.890 (Koltermann and Luthje, 1989), lower than what was observed at the Hudson cruise (Clarke *et al.*, 1984). Swift and Koltermann (1988) give, using the same data, the GSBW salinity as 34.8925. Because of these low values we have used the uncorrected Hudson Data report.

Changes in the deep salinity maximum layer in the Greenland Sea

Not just the deepest waters of the Greenland Sea have changed over the last 15 years: the waters in the deep salinity maximum layer have become more saline. While the salinity in this layer along the western boundary has increased from 34.910 (Meteor) in 1982 to 34.912 (Polarstern) in 1993, the increase in the centre of the gyre has been from 34.895 (Hudson) in 1982 to 34.904 (Valdivia) in 1993. Since convection does not appear to have reached deeper than 2000 m in the last 15 years these changes can only arise through horizontal advection and vertical diffusion.

If the water at the Greenland continental slope is renewed by the outflow from the Arctic Ocean its salinity should remain fairly constant. The Meteor stations from 1982 give a salinity at the rim of about 34.910. However, the Meteor data set gives lower salinities for the GSBW compared to the Hudson data set and may be low. The assumption of a constant salinity at the

rim related to the outflow of EBDW should therefore be justified. This implies that the salinity difference in the salinity maximum layer between rim and centre of the gyre would have been 0.017 in 1982. We therefore put the mean salinity difference ΔS_R to 0.013.

The change of salinity in the layer equals the divergence of advective flux plus the divergence of vertical flux. We approximate the Greenland Sea gyre to a cylinder with the radius R of 150 km and put the thickness D of the salinity maximum layer to 800 m. We also assume that the inflow from the rim takes place through one-quarter of the circumference and the outflow through one-quarter of the circumference at the opposite side. The flow through the gyre can then be likened with the flow through a tube (Fig. 9). The expression for the salinity change $\Delta S_M = 0.009$ of the salinity maximum layer then becomes:

$$\frac{D\pi R^2 \Delta S_M}{t} = uD\frac{\pi R}{2}\Delta S_R - 2\pi R^2 \kappa_v \frac{\partial S}{\partial z} \qquad (3)$$

The diffusion downward has already been estimated and we assume that an upward diffusive flux of similar magnitude occurs. This is a strong assumption. Even if the diffusion coefficient obtained for the deep water can be applied, the salinity of the overlaying water will depend upon the salinity of the overlying water mass. Since convection could reach down to 2000 m either low salinity Arctic Intermediate Water created locally by convection or more saline CBDW advected from the rim could be present. This would affect the gradients and the fluxes. We simply ignore this uncertainty.

By introducing the values for the salinity differences proposed above and the derived value of the diffusion coefficient we find that the generalised velocity through the Greenland Sea gyre becomes $u = 0.15\ cm^{-1}$. This corresponds to an inflow of 0.3 Sv and the salinity maximum layer within the central cylinder is replaced in about 6 years.

The diffusion from above decreases and the diffusion from below increases the density of the salinity maximum layer and a level where the density of the salinity maximum layer is conserved must exist. This level has been displaced downward in recent years, which must be due, perhaps mainly, to the export of GSBW but also to a weakening of the doming of the density surfaces and the circulation of the Greenland Sea central gyre.

The reduction of the volume of the GSBW implies an outflow of 0.2 Sv, which in the absence of an outflow just north of Jan Mayen must pass across the Mohn Ridge into the Norwegian Sea or northward into the Boreas Basin. When the convection is absent, the GSBW is not renewed but rather replaced by a corresponding volume of the temperature maximum water of the CBDW. The deep water of the central Greenland Sea would then be ventilated at a rate of 0.5 Sv regardless if convection occurs or not.

Possible effects of recent observed changes in the waters of the Arctic Mediterranean

Even if no deep convection has occurred recently in the Greenland Sea the AIW can provide overflow water for the Denmark Strait dense enough to resupply the North Atlantic Deep Water. Moreover, in addition to the known source of overflow water in the Iceland Sea (Swift *et al.*, 1980; Swift and Aagaard, 1981), there are several upstream sources capable of producing sufficiently dense water for the overflow like the Arctic Ocean shelves and the Barents Sea inflow to the Arctic Ocean. Also that part of the Atlantic Return Current, which after its recirculation in Fram Strait interacts with the AIW of the Greenland Sea (Strass *et al.*, 1993) is as dense as the main overflow water. A shutdown of the Greenland Sea deep water production is thus primarily of importance for the deep circulation internal to the Arctic Mediterranean, where now the Arctic Ocean sources appear to dominate (Rudels, 1995).

Will a reduction of the Greenland Sea deep water formation have any influence on the inflow of Atlantic Water to the Arctic Mediterranean? A lower convective activity implies a smaller demand of Atlantic Water and the northernmost part of the global thermohaline circulation could then be weakened. However, after at least 10–15 years with reduced convective activity the Greenland Sea surface water is warmer and more saline than before and its seasonal ice cover is less developed. The Atlantic Layer of the Arctic Ocean has also revealed higher temperatures than have previously been recorded (Quadfasel *et al.*, 1991; Carmack *et al.*, 1995).

High temperatures both in the Arctic Ocean and in the upper layers in the Greenland Sea (D. Quadfasel, pers. comm.) can only mean that either the Atlantic inflow or its temperature (or both) has increased or that the heat is no longer removed at the same rate as before. None of these explanations suggest that the benevolent oceanic influence on the climate of north-western Europe should be disappearing.

A situation which could, hypothetically, also close the formation of AIW would be a weakening of the Polar Front. This could permit a massive flow of low salinity Polar Surface Water into the central Greenland Sea (Stigebrandt, 1985; Dickson *et al.*, 1988; Aagaard and Carmack, 1989) and would limit the convection to the low salinity layer and create a low salinity surface layer similar to that of the Arctic Ocean allowing for a stronger ice formation. Clarke *et al.* (1990) believed this to have happened in 1982 when the convection was limited to the upper 200 m.

If such a situation were to persist the southern edge of the Arctic Ocean ice cover would move into the

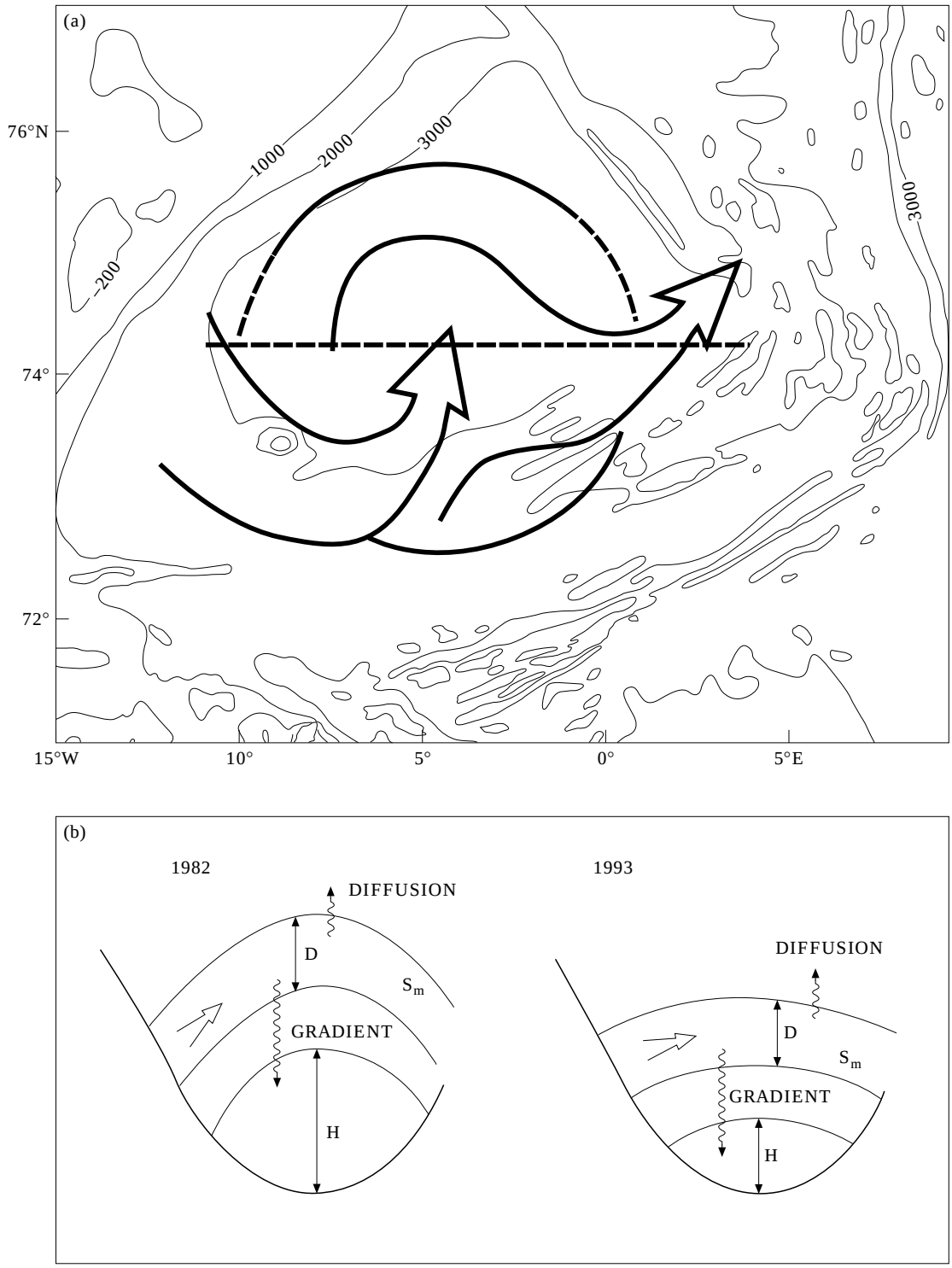

Figure 10. (a) Schematics describing the penetration of EBDW into the central Greenland Sea. (b) The changes in the stratification.

Greenland Sea and the haline convection would, as in the Arctic Ocean, be permanently limited to the upper low salinity layer (Stigebrandt, 1985). The small ice formation in the Greenland Sea in 1994 (D. Quadfasel, pers. comm.) indicates that such a situation is not in the process of being established as yet.

Acknowledgements

We wish to thank Norbert Verch for technical assistance. Financial support for BR was given by the Deutsche Forschungsgemeinschaft, SFB 318. The Valdivia 136 cruise was supported by the Commission of the European Community under the Mast II programme (Contract MAS-TTCT 93-0057).

References

Aagaard, K., Coachman, L. K., and Carmack, E. C. 1981. On the halocline of the Arctic Ocean. Deep-Sea Research, 28: 529–545.

Aagaard, K., Swift, J. H., and Carmack, E. C. 1985. Thermohaline circulation in the Arctic Mediterranean Seas. Journal of Geophysical Research, 90: 4833–4846.

Aagaard, K., and Carmack, E. C. 1989. The role of sea ice and other fresh water in the Arctic circulation. Journal of Geophysical Research, 94: 14 485–14 498

Aagaard, K., Fahrbach, E., Meincke, J., and Swift, J. H. 1991. Saline outflow from the Arctic Ocean: its contribution to the deep waters of the Greenland, Norwegian and Iceland seas. Journal of Geophysical Research, 96: 20 433–20 441.

Aagaard, K., and Carmack, E. C. 1994. The Arctic Ocean and climate: a perspective. *In* The role of the Polar Oceans in Shaping the Global Climate, pp. 33–46. Ed. by O. M. Johannessen, R. D. Muench and J. E. Overland. American Geophysical Union, Washington.

Anderson, L. G., Björk, G., Holby, O., Jones, E. P., Kattner, G., Koltermann, K.-P., Liljeblad, B., Lindegren, R., Rudels, B., and Swift, J. H. 1994. Water masses and circulation in the Eurasian Basin: results from the Oden 91 Expedition. Journal of Geophysical Research, 99: 3273–3283.

Backhaus, J. O. 1995. Prozestudien zur Ozeanischen Konvektion. Habilitationsabhandlung der Universität Hamburg. 112 pp.

Blindheim, J. 1989. Cascading of Barents Sea bottom water into the Norwegian Sea. Rapports et Prorès-verbaux des Réunions du Conseil International pour l'Exploration de la Mer, 188: 49–58.

Bourke, R. H., Weigel, A. M., and Paquette, R. G. 1988. The westward turning branch of the West Spitsbergen Current. Journal of Geophysical Research, 93: 14 065–14 077.

Buch, E., Malmberg, S.-A., and Kristmannsson, S. S. 1992. Arctic Ocean deep water masses in the western Iceland Sea. ICES CM 1992/C, Hydrography Committee, 18 pp.

Buch, E., Malmberg, S.-A., and Kristmannsson, S. S. 1996. Arctic Ocean deep water masses in the western Iceland Sea. Journal of Geophysical Research, 101: 11 965–11 973.

Carmack, E. C. 1986. Circulation and mixing in ice covered waters. *In* The Geophysics of Sea Ice, pp. 641–712. Ed. by N. Untersteiner. Plenum, New York.

Carmack, E. C. 1990. Large-Scale physical oceanography of Polar Oceans. *In* Polar Oceanography, Part A, pp. 171–212. Ed. by W. O. Smith, Jr. Academic Press, San Diego, California.

Carmack, E. C., and Aagaard, K. 1973. On the deep water of the Greenland Sea. Deep-Sea Research, 20: 687–715.

Carmack, E. C., Macdonald, R. W., Perkin, R. G., McLaughlin, F. A., and Pearson, R. J. 1995. Evidence for warming of Atlantic Water in the southern Canadian Basin of the Arctic Ocean: results from the Larsen-93 expedition, Geophysical Research Letters, 22: 1061–1064.

Clarke, R. A., Reid, J. L., and Swift, J. H. 1984. CSS Hudson Cruise 82-001. SIO reference 84-14. Scripps Institute of Oceanography.

Clarke, R. A., Swift, J. H., Reid, J. L., and Koltermann, K.-P. 1990. The formation of Greenland Sea Deep Water: double-diffusion or deep convection? Deep-Sea Research, 37: 687–715.

Coachman, L. K., and Aagaard, K. 1974. Physical oceanography of the Arctic and Sub-Arctic Seas. *In* Marine Geology and Oceanography of the Arctic Ocean, pp. 1–74. Ed. by Y. Herman. Springer, New York.

Dickson, R. R., Meincke, J., Malmberg, S.-A., and Lee, A. J. 1988. The "Great Salinity Anomaly" in the Northern North Atlantic 1968–1982. Progress in Oceanography, 20: 103–151.

Garwood, R. W., Isakari, S. M., and Gallacher, P. C. 1994. Thermobaric convection. *In* The Polar Oceans and their Role in Shaping the Global Environment, pp. 199–209. Ed. by O. M. Johannessen, R. D. Muench and J. E. Overland. American Geophysical Union, Washington.

GSP-Group. 1990. The Greenland Sea Project—a venture toward improved understanding of the ocean's role in climate. EOS, 71: 750–751, 754–755.

Helland-Hansen, B., and Nansen, F. 1909. The Norwegian Sea. Its physical oceanography based upon the Norwegian researches 1900–1904. Report on Norwegian Fishery and Marine Investigations II(1), Kristiania.

Houssais, M.-N. 1988. Testing a coupled ice-mixed layer-ocean model under subarctic conditions. Journal of Physical Oceanography, 18: 196–210.

Houssais, M.-N., and Hibler, III W. D. 1993. Importance of convective mixing in seasonal ice margin simulations. Journal of Geophysical Research, 98: 16 427–16 448.

Jones, E. P., Rudels, B., and Anderson, L. G. 1995. Deep waters of the Arctic Ocean: origins and circulation. Deep-Sea Research, 42: 737–760

Jones, H., and Marshall, J. 1993. Convection and rotation in a neutral ocean. A study of open ocean deep convection. Journal of Physical Oceanography, 23: 1009–1039.

Killworth, P. D. 1983. Deep convection in the world ocean. Reviews in Geophysics and Space Physics, 21: 1–26.

Koltermann, K. P., and Lüthje, H. 1989. Hydrographic Atlas of the Greenland and Northern Norwegian Seas (1979–1987). Deutsches Hydrographisches Institut, No. 2328, Hamburg.

Ledwell, J. R., Watson, A. J., and Law, C. S. 1993. Evidence for slow mixing across the pycnocline from an open ocean tracer-release experiment. Nature, 364: 701–703.

Lemke, P. 1987. A coupled one-dimensional sea ice-ocean model. Journal of Geophysical Research, 92: 13 164–13 172

Loeng, H., Ozhigin, V., Ådlandsvik, B., and Sagen, H. 1993. Current measurements in the north-eastern Barents Sea. ICES CM 1993/C:41, Hydrographic Committee, 22 pp.

Malmberg, S. A. 1983. Hydrographic investigations in the Iceland and Greenland Seas in late winter 1971. "Deep Water Project". Jökull, 33: 133–140.

McCartney, M. S., and Talley, L. D. 1984. Warm-to-cold water conversions in the northern North Atlantic Ocean. Journal of Physical Oceanography, 14: 922–935.

McDougall, T. J. 1983. Greenland Sea bottom water formation: a balance between advection and double-diffusion. Deep-Sea Research, 30: 1109–1117

Meincke, J., Jonsson, S., and Swift, J. H. 1992. Variability of convective conditions in the Greenland Sea. ICES Marine Science Symposia, 195: 32–39.

Meincke, J., and Rudels, B. 1996. Greenland Sea deep water: a balance between convection and advection. Proceedings of ACSYS Conference, Göteborg, 7–11 November 1994, WMO TD 760: 436–440.

Midttun, L. 1985. Formation of dense bottom water in the Barents Sea. Deep-Sea Research, 32: 1233–1241.

Munk, W. H. 1966. Abyssal recipes. Deep-Sea Research, 13: 709–730.

Nansen, F. 1906. Northern waters. Captain Roald Amundsen's oceanographic observations the Arctic seas in 1901. Vid-selskap Skrifter I, Mat.-Naturv. kl. Dybvad Christiania 1 (3) 145 pp.

Niiler, P. P., and Kraus, E. B. 1977. One-dimensional models of the upper ocean. *In* Modelling and prediction of the upper layers of the ocean, pp. 143–179. Ed. by I. E. Kraus. Pergamon Press, Oxford.

Quadfasel, D., and Meincke, J. 1987. Note on the thermal structure of the Greenland Sea gyres. Deep-Sea Research, 34: 1883–1888.

Quadfasel, D., Gascard, J.-C., and Koltermann, P. K. 1987. Large-scale oceanography in Fram Strait during the 1984 Marginal Ice Zone experiment. Journal of Geophysical Research, 92: 6719–6728.

Quadfasel, D., Sy, A., Wells, D., and Tunik, A. 1991. Warming in the Arctic. Nature, 350: 385.

Quadfasel, D., Rudels, B., and Selchow, S. 1992. The Central Bank vortex in the Barents Sea: water mass transformation and circulation. ICES Marine Science Symposia, 195: 40–51.

Quadfasel, D., Sy, A., and Rudels, B. 1993. A ship of opportunity section to the North Pole: upper ocean temperature observations. Deep-Sea Research, 40: 777–789.

Rhein, M. 1991. Ventilation rates of the Greenland and Norwegian Seas derived from distributions of the chlorofluoromethanes F11 and F12, Deep-Sea Research, 38: 485–503

Roach, A., Aagaard, K., and Carsey, F. 1993. Coupled ice-ocean variability in the Greenland Sea. Atmosphere and Ocean, 31: 319–337.

Rudels, B. 1986. The Θ–S relations in the northern seas: implications for the deep circulation. Polar Research, 4: 133–159.

Rudels, B. 1987. On the mass balance of the Polar Ocean, with special emphasis on the Fram Strait. Norsk Polarinstitutt Skrifter 188: 53 pp.

Rudels, B. 1993. High latitude ocean convection. *In* Flow and Creep in the Solar System: Observations, Modelling and Theory, pp. 323–356. Ed. by D. B. Stone and S. K. Runcorn. Academic Publishers, Dordrecht.

Rudels, B. 1995. The thermohaline circulation of the Arctic Ocean and the Greenland Sea. Philosophical Transactions of the Royal Society of London A, 352: 287–299.

Rudels, B., Quadfasel, D., Friedrich, H., and Houssais, M.-N. 1989. Greenland Sea convection in the winter of 1987–1988. Journal of Geophysical Research, 94: 3223–3227.

Rudels, B., Meincke, J., Friedrich, H., and Schulze, K. 1993. Greenland Sea deep water: a report on the 1993 winter and spring cruises by RVs Polarstern and Valdivia. ICES CM 993/C:59, Hydrography Committee 10 pp.

Rudels, B., Jones, E. P., Anderson, L. G., and Kattner, G. 1994. On the intermediate depth waters of the Arctic Ocean. *In* The role of the Polar Oceans in Shaping the Global Climate, pp. 33–46. Ed. by O. M. Johannessen, R. D. Muench and J. E. Overland. American Geophyical Union, Washington.

Rudels, B., Anderson, L. G., and Jones, E. P. 1996. Formation and evolution of the surface mixed layer and the halocline of the Arctic Ocean. Journal of Geophysical Research, 101: 8807–8821.

Sælen, O. H. 1986. On the exchanges of bottom water between the Greenland Sea and Norwegian Seas. *In* Nordic perspectives on Oceanography, pp. 33–44. Ed. by P. Lundberg. Acta Geophysica 3, Göteborg, Sweden.

Schauer, U., Muench, R. D., Rudels, B., and Timokhov, L. 1997. The impact of eastern Arctic shelf water on the Nansen Basin intermediate layers. Journal of Geophysical Research C2, 102: 3371–3382.

Schlosser, P., Böhnisch, G., Rhein, M., and Bayer, R. 1991. Reduction of deep water formation in the Greenland Sea during the 1980s: evidence from tracer data. Science, 251: 1054–056.

Steele, M., Morison, J. H., and Curtin, T. B. 1995. Halocline formation in the Barents Sea. Journal of Geophysical Research, 100: 881–894.

Stigebrandt, A. 1985. On the hydrographic and ice conditions in the northern North Atlantic during different phases of a glaciation cycle, Palaeogeography, Palaeoclimatology and Palaeoecology 50: 303–321.

Strass, V. H., Fahrbach, E., Schauer, U., and Sellmann, L. 1993. Formation of Denmark Strait overflow water by mixing in the East Greenland Current. Journal of Geophysical Research, 98: 6907–6919.

Swift, J. H., Aagaard, K., and Malmberg, S.-A. 1980. The contribution of the Denmark Strait overflow to the deep North Atlantic. Deep-Sea Research, 27: 29–42.

Swift, J. H., and Aagaard, K. 1981. Seasonal transitions and water mass formation in the Icelandic and Greenland Seas. Deep-Sea Research, 28: 1107–1129.

Swift, J. H., and Koltermann, K. P. 1988. The origin of Norwegian Sea Deep Water. Journal of Geophysical Research, 93: 3563–3569.

Untersteiner, N. 1988. On the ice and heat balance in Fram Strait. Journal of Geophysical Research, 92: 527–532.

Visbeck, M., Fischer, J., and Schott, F. 1995. Preconditioning the Greenland Sea for deep convection: ice formation and ice dirft. Journal of Geophysical Research, 100: 18 489–18 502.

Walin, G. 1993. On the formation of ice on deep weakly stratified water. Tellus, 45A: 143–157.

Worthington, L. V. 1953. Oceanographic results of Project Skijump I and II. Transactions of the American Geophysical Union, 34: 543–551.

Worthington, L. V. 1970. The Norwegian Sea as a mediterranean basin. Deep-Sea Research, 17: 77–84.